Environmental Science & Technology Letters

Letter

pubs.acs.org/journal/estlcu

Glycosphingolipids Enhance Bacterial Attachment and Fouling of Nanofiltration Membranes

Robert Haas,[†,§] Jenia Gutman,[†] Nathaniel C. Wardrip,[†] Kazuyoshi Kawahara,[‡] Wolfgang Uhl,[§,∥] Moshe Herzberg,[†] and Christopher J. Arnusch*[,†]

[†]Department of Desalination and Water Treatment, Zuckerberg Institute for Water Research, Jacob Blaustein Institutes for Desert Research, Ben-Gurion University of the Negev, Sede-Boqer Campus, Beer Sheva 84990, Israel

[‡]Department of Biosciences, College of Science and Engineering, Kanto Gakuin University, Yokohama, Japan

[§]Chair of Water Supply Engineering, Technische Universität Dresden, 01062 Dresden, Germany

[∥]Norwegian Institute for Water Research (NIVA), 0349 Oslo, Norway

Supporting Information

ABSTRACT: Biofouling is a ubiquitous problem in many places in society and technology, especially in reverse osmosis or nanofiltration (NF) processes. Initial stages in the development of the biofilm include attachment of bacteria to the surface, where bacterial outer membrane components such as biopolymers, lipids, and proteins play important roles. Here we show that the glycosphingolipid (GSL) unique to *Sphingomonas* species is a key player in the initial attachment of bacteria to NF membranes whereas lipopolysaccharide (LPS), the major glycolipid in many Gram-negative species, is less significant. GSL and LPS were deposited on an NF membrane with subsequent bacterial culture injection in a three-dimensionally printed microfluidic flow cell. Flux, rejection, and pressure changes showed that GSL caused permanent membrane fouling. This study underlines the significance of *Sphingomonas* for the initial attachment of bacteria to membranes. A deeper understanding and identification of key components in the biofouling process may help define strategies for biofilm prevention.

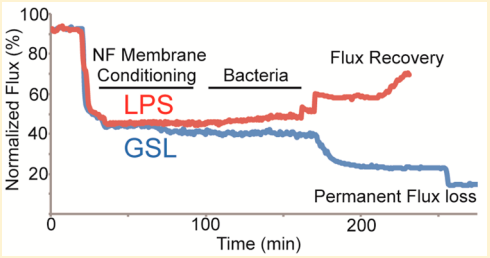

INTRODUCTION

Reverse osmosis (RO) and nanofiltration (NF) membrane modules are integral components in water purification and other separation processes,[1,2] yet this technology suffers from fouling, which includes biofilm formation in the module and on the polyamide surfaces of the membrane.[3−6] New solutions are urgently needed to mitigate the initiation, growth, or dispersion of biofilms.[7,8] Understanding the causes and mechanisms of biofilm initiation on RO or NF membranes may lead to better process management, improved process design, and the development of biofilm resistant membranes.[9,10]

Microbial community structure analyses of biofilms on membranes have led to a deeper understanding of the entire bacterial community in the biofilm.[11,12] Recently, Bereshenko et al. identified *Sphingomonas* species (spp.) as a possible initiator and/or dominator species.[13] The study revealed that *Sphingomonas* spp. formed a thin base layer on RO membrane surfaces under normal operating conditions to which other biofilm-forming bacteria attached. *Sphingomonas* spp. have been identified in water, soil, and sediments and are present in diverse water treatment and supply systems.[14] The outer membrane of *Sphingomonas* consists essentially of glycosphingolipids[15] (GSLs) and is uniquely different from those of the majority of Gram-negative bacteria, in which lipopolysaccharides (LPSs) dominate. The outer bacterial membrane physically mediates adhesion of cells to a surface,[16,17] and therefore, these glycolipids likely play a critical role in the initial stages of attachment and biofilm formation on RO and NF membrane surfaces.

To reveal the possible contribution of GSL and LPS to NF system performance and bacterial adhesion, in this study we compared vesicles consisting of GSL to vesicles consisting of LPS deposited on NF membranes using a microfluidic cross-flow cell. The apparatus led to repeatable and accurate measurement of membrane performance, flux, and fouling. The reversibility of fouling of each component as well as its ability to condition the membrane surface for bacterial attachment and consequent fouling was shown. Taken together, the observed GSL behavior delineates involved mechanisms that include *Sphingomonas* spp. in RO and NF biofouling phenomena.

MATERIALS AND METHODS

Three-Dimensionally Printed Microfluidic Cross-Flow Device. The microfluidic cross-flow device was printed on a Connex printer (Stratasys) using PolyJet multimaterial three-dimensional printing technology (Figure S1, Supporting

Received: December 25, 2014
Revised: January 27, 2015
Accepted: January 28, 2015

DOI: 10.1021/ez500409h
Environ. Sci. Technol. Lett. XXXX, XXX, XXX−XXX

Information). The body of the device was printed in a hard clear polymer Veroclear, and a thin overcoating was printed using a black rubbery polymer Tangoblackplus to prevent leakage. The microchannel was 30 mm long, 1.4 mm wide, and 0.1 mm deep. The permeate tubing was glued into place with epoxy, and the feed inlet and exit were threaded by tapping. Rectangular membrane coupons (4.5 cm × 1.5 cm, NF 200 manufactured by Filmtec) were washed by being soaked in 70% ethanol for 3 × 5 min and then soaked in deionized (DI) water in a sonication bath for 3 × 10 min. The membranes were stored in DI water at 4 °C until they were used further. The membrane was inserted into the device, and six bolts were tightened by hand. The device was connected to the pump, and a DI water flow of 1 mL/min was initiated, after which the bolts were fully tightened using a wrench. A valve was placed after the retentate exit point for dead-end or cross-flow modes. The permeate mass flow was measured using a μ-Flow meter (Bronkhorst, Ruurlo, The Netherlands). Conductivity was measured by a custom-built electrode cell with a volume of 5 μL and a cell constant of 11.9 cm^{-1}.[18] For the NF 200 membrane, flow rates of 0.08−0.4 mL/min were tested at hydraulic pressures of 3.8−4.2 bar and gave permeate flow rates of 0.98−1.2 g/h (23−29 LMH). For the cross-flow configuration, the system was adjusted to operate at 4 bar and gave a permeate recovery of 10%. Because the cross-sectional area of the channel was 1.4×10^{-3} cm^2, the flow rate of 0.18 mL/min corresponded to a relatively low channel linear velocity of 2.1 cm/s and a Reynolds number of 4. However, the microfluidic geometry gave a high shear rate of 1260 s^{-1}. NF 200 membrane samples (n = 21) were tested for salt rejection (10 mM $MgSO_4$) and gave an average of 94.1 ± 2.5% rejection. Coupons falling outside this range were not used in the experiments.

Lipid Preparation. Lipopolysaccharides (rough strains) from *Salmonella enterica* serotype minnesota Re 595 (Re 145 mutant) were purchased from Sigma-Aldrich (Israel, catalog no. 146 L9764). GSL-1 was obtained from the bacteria *Sphingomonas paucimobilis* IAM12576, extracted with the chloroform/methanol method,[19] followed by elution from a silica gel column via a stepwise increase in the methanol fraction. GSL-1 was deemed to be pure by thin layer chromatography and its identity confirmed using matrix-assisted laser desorption ionization time-of-flight mass spectrometry, where no other lipid could be detected. Lipid vesicles were prepared using a recently published method.[20] Lipid solutions were based on weight, where 0.2 mg of lipids was prepared in 1 mL of 200 mM NaCl. For fluorescent labeling of vesicles, 1,2-dimyristoyl-*sn*-glycero-3-phosphoethanolamine-*N*-(lissamine rhodamine B sulfonyl) (ammonium salt) (Rh-PE) was added (1%) (PL 810157P, Avanti-Polar Lipids, Alabaster, AL).

Preparation of Bacteria. *Pseudomonas fluorescens* mut 3 was used, which was grown in Luria-Bertani (LB) medium or agar plates with kanamycin sulfate (Sigma, 25 mg/L) for 48 h at 30 °C. The bacteria were pelleted by centrifugation (4000g at 4 °C for 10 min), and the pellet was washed three times and finally resuspended at an OD_{600} of 0.1 in an aqueous solution of NaCl (200 mM). For assessing viable bacteria present on the membrane, the treated membrane sample was cut to the channel size and placed in an aqueous solution of NaCl (25 mL, 200 mM). The mixture was vortexed at the highest speed for 10 min, and from this solution, viable colonies were counted on agar plates after incubation for 48 h.

Hydrophobicity and Hydrophilicity of the GSL and LPS Vesicle Layer: Contact Angle Measurements. The contact angles were measured using a sessile drop of DI water on an OCA-20 contact angle analyzer (DataPhysics, Filterstadt, Germany). Membrane samples were dried in a vacuum desiccator for at least 3 h at room temperature and fixed on a glass slide with double-sided tape. An average with the standard deviation was measured from 6 drops (0.3 μL of DI water) on each membrane sample.

Microscopy. Fluorescent lipids on membrane samples were observed using an inverted microscope (Zeiss AXIO Imager) with excitation at 560 nm and emission at 583 nm.

Performance Testing before and after the Membranes Had Been Conditioned with GSL or LPS Vesicles and Subsequent Bacterial Adhesion. *Flowcell/Membrane Preparation (cross-flow).* A standard experimental procedure was developed that consisted of the following. First, the membrane performance was tested with DI water at a rate of 0.18 mL/min as the feed solution at a constant pressure of 4 bar, which gave a permeate rate of ∼1.2 g/h. After a constant permeate flow rate was observed, the feed solution was changed to $MgSO_4$ (10 mM) using the same settings and salt rejection was assessed by measuring the conductivity of the feed and the permeate solutions. Only membranes with average rejection values of 94.1 ± 2.5% were used. Next, the system was purged with DI water for 35 min using a flow rate of 1 mL/min at 4.2 bar, and then the rate was returned to 0.18 mL/min.

Injection of Lipid and/or Bacteria (dead-end). The system was changed from a cross-flow system to a dead-end system by closing the valve at the retentate exit. For lipid only conditioning experiments, lipids (1 mL, in 200 mM NaCl) were injected at a rate of 0.1 mL/min until a pressure of 4.7 bar was reached, after which the flow rate was reduced to 0.013 mL/min, corresponding to the permeate flow seen previously with the $MgSO_4$ feed solution mentioned above. For experiments with lipid and bacteria, lipids (1 mL, in 200 mM NaCl) and subsequently bacteria (1 mL, in 200 mM NaCl) were injected under the same parameters that were used for the lipid only experiments. The pressure was recorded every 2 min.

Feed Solutions after Membrane Conditioning (cross-flow). The system was switched back to cross-flow mode, and membrane performance was tested again using $MgSO_4$ (10 mM, flow rate of 0.18 mL/min, 4 bar) as a feed solution. Finally, the feed solution was changed to an aqueous solution of NaCl (7 mM) and $CaCl_2$ (1 mM) and the permeate flow recorded. Mean values of three to five experiments are reported.

RESULTS AND DISCUSSION

Lipid Fouling Behavior on NF Membranes. A system that consisted of a syringe pump, pressure and flow meters, and a microfluidic flow cell with a possibility for cross-flow or dead-end operation was designed (Figure S1, Supporting Information).[18] Parameters were chosen to imitate actual NF filtration conditions, within the limitations of the test apparatus. $MgSO_4$ was used because of its high rejection by NF membranes compared to the low rejection of NaCl. Magnesium cations have cross-linking activity lower than that of calcium, and therefore when calcium is added, chelation effects may be detected. For testing the fouling behavior of GSL versus LPS vesicle layers, a membrane was placed in the cell with a DI water feed solution until a stable flux was achieved (∼30 min) (Figure 1). Then, the feed solution was changed to $MgSO_4$ (10

DOI: 10.1021/ez500409h
Environ. Sci. Technol. Lett. XXXX, XXX, XXX−XXX

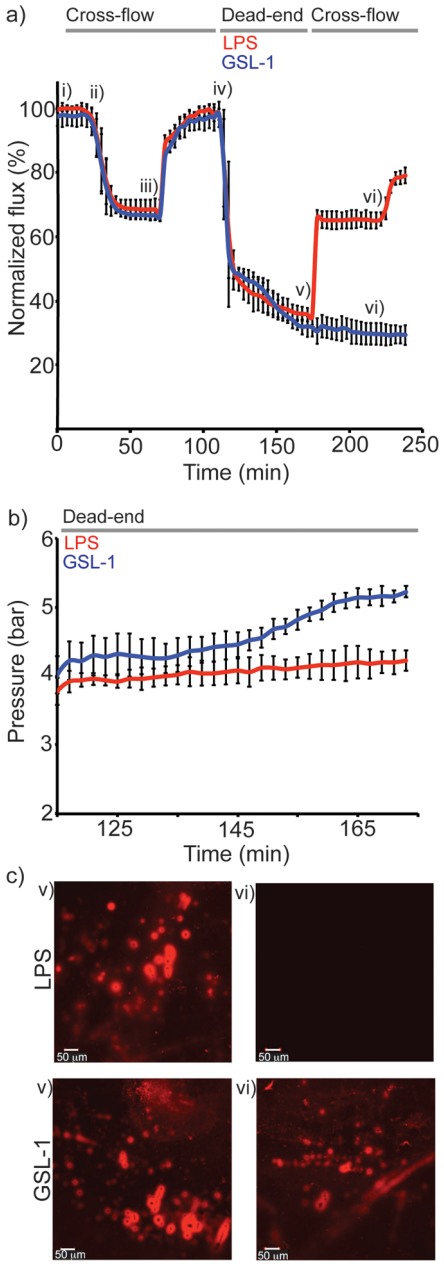

Figure 1. (a) Performance of NF200 membranes (red for the LPS-deposited membrane and blue for the GSL-deposited membrane) under experimental conditions: (i) cross-flow (DI, 0.18 mL/min, 4 bar), (ii) cross-flow (10 mM $MgSO_4$, 0.18 mL/min, 4 bar), (iii) cross-flow (DI, 1 mL/min, then 0.18 mL/min, 4.2 bar), (iv) dead-end, LPS or GSL (200 mM NaCl, 0.013 mL/min), (v) cross-flow (10 mM $MgSO_4$, 0.18 mL/min, 4 bar), and (vi) cross-flow (7 mM NaCl and 1 mM $CaCl_2$, 0.18 mL/min, 4 bar). (b) Pressure monitored upon lipid injection (dead-end mode) (red for the LPS-deposited membrane and blue for the GSL-deposited membrane). (c) Fluorescence microscopy images of membranes at points v and vi for LPS (top) and GSL (bottom). Reported mean values from five replicate runs with the standard deviation are shown.

mM) for the purpose of measuring NF membrane performance, and rejection measurements were performed (Figure 1a, ii). Because of the elevated osmotic pressure of the feed solution, the permeate rate decreased to 68% of the original flux. Afterward, the feed was returned to DI water for complete removal of $MgSO_4$ and the permeate flux returned to the initial rate. At this point, the lipid solutions were injected into the system in a dead-end configuration so that the entire amount of lipids would be concentrated at the membrane surface (Figure 1a, iv). The lipids were injected at a constant membrane flux (18.6 LMH), and the pressure was monitored over the entire injection (Figure 1b). We observed a significantly larger pressure increase for GSL (maximal pressure of 5.2 ± 0.2 bar) than for LPS (maximal pressure of 4.1 ± 0.2 bar). This result gave an initial indication that the GSL membrane fouling mechanism was different from that of LPS and presented a stronger resistance to permeation. After lipid injection, the system was switched back to cross-flow operation, and performance was measured using $MgSO_4$ (10 mM) as the feed solution (Figure 1a, v). At this point in the experiment, a permanent flux decline was observed with the membrane fouled with GSL. Specifically, GSL was not removed because of cross-flow operation with a 10 mM $MgSO_4$ solution; the flux remained at a value of 30% of the initial flux (~0% permeate flux recovery), while almost 100% permeate flux recovery was observed during cross-flow operation after LPS was deposited. It should be mentioned that salt rejection values did not change with respect to the initial rejection of the pristine membrane and remained constant (95.6 ± 0.2% for 10 mM $MgSO_4$). Finally, the feed was changed from $MgSO_4$ (10 mM) to a mixture of 7 mM NaCl and 1 mM $CaCl_2$ (Figure 1a, vi). A decreased osmotic pressure difference between the feed and permeate solutions leading to a higher permeate flux was expected because of the lower ionic strength of the feed solution in combination with the low NF membrane rejection of NaCl (~34%). Indeed, a higher flux was observed for LPS-treated membranes; however, the flux did not change for membranes treated with GSL. This indicated a permanent GSL fouling layer on the surface, which likely induced such a high hydraulic resistance that it obscured the reduced osmotic pressure. To visualize these differences, a fluorescent lipid Rh-PE was added to the GSL and LPS vesicles and membranes were observed microscopically at points after lipid deposition, and subsequently after a washing step (Figure 1c). Fluorescently stained membranes were seen before and after washing in the case of GSL deposition, whereas lipids were detected only on LPS-deposited membranes prior to the washing step. After washing, no fluorescence was observed.

Bacterial Attachment and Detachment after Lipid Deposition. Next, a live culture of bacteria was introduced into the system to test the possible effect of *Sphingomonas* GSL on further bacterial attachment. Therefore, a *P. fluorescens* mut 3 suspension was injected (OD_{600} = 0.1, 1 mL of 200 mM NaCl) after GSL or LPS lipid solutions were deposited on the membranes as described above (Figure 2). To achieve similar bacterial loadings on the conditioned membranes, equivalent amounts of bacterial suspension were injected using the dead-end filtration mode, which produced equivalent volumes of permeate. Upon addition of bacteria, the pressure increased to ~6.5 bar in the case of GSL followed by bacteria, compared to ~6 bar for LPS followed by bacteria, and ~4 bar for bacteria alone. The comparable elevated pressures in the cases of lipid followed by bacteria likely corresponded to similar amounts of bacteria attached to the membrane. However, when the system feed solution was switched to cross-flow with $MgSO_4$ (10 mM), opposite trends for GSL and LPS were observed. Permeate flux recovered to 60% of the original pure water flux in the case of treatment with LPS and bacteria and was comparable to 68% of the original pure water flux seen with the control membrane

DOI: 10.1021/ez500409h
Environ. Sci. Technol. Lett. XXXX, XXX, XXX−XXX

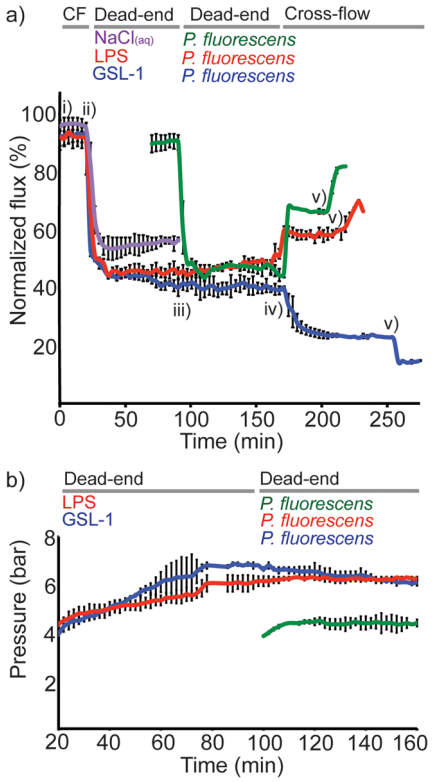

Figure 2. (a) Performance of NF200 membranes [red for the LPS-deposited membrane, blue for the GSL-deposited membrane, purple for the NaCl (200 mM) control membrane, and green for the control with only bacteria) under experimental conditions: (i) cross-flow (CF) (DI water, 0.18 mL/min, 4 bar), (ii) dead-end, LPS or GSL (200 mM NaCl, 0.013 mL/min), (iii) dead-end, *P. fluorescens* mut 3 (OD_{600} of 0.1, 1 mL, 200 mM NaCl, 0.013 mL/min), (iv) cross-flow ($MgSO_4$, 10 mM, 0.18 mL/min, 4 bar), and (v) cross-flow (7 mM NaCl and 1 mM $CaCl_2$, 0.18 mL/min, 4 bar). (b) Pressure monitored upon injection of lipid and bacteria (dead-end mode). Reported mean values from triplicate runs with the standard deviation are shown.

that was treated only with bacteria. In contrast, the flux dropped to ~20% of the original pure water flux for the case of GSL followed by the deposition of bacteria (Figure 2). The additional flux decline could be attributed to an elevated level of NF rejection for $MgSO_4$ (~94%) and the associated increase in the osmotic pressure, which is significantly higher than for the NaCl solution used for lipid and/or bacterial deposition (measured NaCl NF rejection of ~34%). This effect was combined with the firmly attached bacterial layer on the GSL conditioning film. Both effects are required for inducing cake/biofilm enhanced concentration polarization, which consequently reduced permeate flux.[21−23] In the study presented here, only in the case in which deposited bacteria remained during cross-flow would the deposited cells hinder the back diffusion of salt from the membrane surface and result in an increased osmotic pressure difference. Finally, when the feed solution was changed to 7 mM NaCl and 1 mM $CaCl_2$, an increase in flux was seen in the case of LPS with bacteria, and bacteria alone as described above. Unexpectedly, however, a further decrease in flux was seen in the case of GSL with bacteria. A plausible explanation for this effect may be that chelation of Ca^{2+} ions with bacteria or bacterial components, which remain on the membrane in the case of GSL, increases the cake or biological matrix close to the membrane surface.[24] Calcium is known to cross-link soluble and colloidal microbial products such as polysaccharides and biopolymers to form rigid gel layers and interact with especially multiple negatively charged carboxylic acid groups,[25] which could increase the hydraulic resistance of the fouling layer.

We quantitatively verified bacterial attachment by removing membranes from the device at different time points and counting the total number of viable bacterial colonies attached to it. After LPS and GSL deposition followed by bacterial challenge, both GSL- and LPS-treated membranes had equal numbers of bacteria [1.5×10^6 colony-forming units (CFU)], which translates to 3.6×10^4 bacteria/mm^2, or 1 cell/28 μm^2. After the washing step in the cross-flow configuration, no colony-forming units were detected on the membrane for LPS, compared to 1.0×10^6 CFU for GSL (2.4×10^4 bacteria/mm^2 or 1 cell/42 μm^2). This provided evidence that the drop in flux in the GSL-treated membranes may be attributed to a much stronger interaction between the attached viable bacteria and the conditioned surface than in the case of LPS.

The physical properties of the membrane surface were altered via lipid deposition. The untreated, GSL-deposited, and LPS-deposited membranes gave pure water contact angles of 36 ± 1°, 51 ± 2°, and 26 ± 2°, respectively. Hydrophilic membranes are known to be more resistant to fouling, interacting less with hydrophobic organics in the effluent.[26] Membrane surfaces were made more hydrophobic after GSL deposition, which sheds light on an important aspect of the mechanism of the attachment of bacteria to GSL vesicles and thus *Sphingomonas*-coated surfaces. Overall, this study highlights the importance of GSL and *Sphingomonas* spp. in the initial stages of bacterial attachment on NF membrane surfaces. Both the irreversible interaction of GSL with the membrane surface and providing bacteria with an excellent conditioning film for further attachment are important factors for supporting or enhancing subsequent biofouling. Further studies that aim to elucidate biophysical aspects of membrane-adhered foulants and a clearer understanding of the mechanisms of bacterial attachment will be an important guide for novel biofilm mitigation strategies.

■ ASSOCIATED CONTENT

Ⓢ Supporting Information

Schematic of apparatus, including the design of the three-dimensionally printed microfluidic flow cell. This material is available free of charge via the Internet at http://pubs.acs.org.

■ AUTHOR INFORMATION

Corresponding Author

*Telephone: 972-8-656-3532. Fax: 972-8-656-3503. E-mail: arnusch@bgu.ac.il.

Notes

The authors declare no competing financial interest.

■ ACKNOWLEDGMENTS

This research was supported by The Israel Science Foundation (Grant 1474-13) to C.J.A. R.H. thanks the German Ministry for Education and Research (BMBF) for funding his stay in Israel in the framework of the Young Scientists Exchange Program (YSEP) under Grant YSEP86. We are grateful to Stratasys (Rehovot, Israel) for collaboration in fabrication of the three-dimensionally printed cross-flow device.

DOI: 10.1021/ez500409h
Environ. Sci. Technol. Lett. XXXX, XXX, XXX−XXX

REFERENCES

(1) Shannon, M. A.; Bohn, P. W.; Elimelech, M.; Georgiadis, J. G.; Mariñas, B. J.; Mayes, A. M. Science and technology for water purification in the coming decades. *Nature* **2008**, *452*, 301−310.

(2) Elimelech, M.; Phillip, W. A. The future of seawater desalination: Energy, technology, and the environment. *Science* **2011**, *333*, 712−717.

(3) Matin, A.; Khan, Z.; Zaidi, S. M. J.; Boyce, M. C. Biofouling in reverse osmosis membranes for seawater desalination: Phenomena and prevention. *Desalination* **2011**, *281*, 1−16.

(4) Gutman, J.; Fox, S.; Gilron, J. Interactions between biofilms and NF/RO flux and their implications for control: A review of recent developments. *J. Membr. Sci.* **2012**, *421*−*422*, 1−7.

(5) Flemming, H.-C.; Wingender, J. The biofilm matrix. *Nat. Rev. Microbiol.* **2010**, *8*, 623−633.

(6) Flemming, H.-C. Biofouling in water systems: Cases, causes and countermeasures. *Appl. Microbiol. Biotechnol.* **2002**, *59*, 629−640.

(7) Rahaman, M. S.; Thérien-Aubin, H.; Ben-Sasson, M.; Ober, C. K.; Nielsen, M.; Elimelech, M. Control of biofouling on reverse osmosis polyamide membranes modified with biocidal nanoparticles and antifouling polymer brushes. *J. Mater. Chem. B* **2014**, *2*, 1724−1732.

(8) Bar-Zeev, E.; Elimelech, M. Reverse Osmosis Biofilm Dispersal by Osmotic Back-Flushing: Cleaning via Substratum Perforation. *Environ. Sci. Technol. Lett.* **2014**, *1*, 162−166.

(9) Geise, G. M.; Lee, H.-S.; Miller, D. J.; Freeman, B. D.; McGrath, J. E.; Paul, D. R. Water purification by membranes: The role of polymer science. *J. Polym. Sci., Part B: Polym. Phys.* **2010**, *48*, 1685−1718.

(10) Lei, J.; Ulbricht, M. Macroinitiator-mediated photoreactive coating of membrane surfaces with antifouling hydrogel layers. *J. Membr. Sci.* **2014**, *455*, 207−218.

(11) Bereschenko, L. A.; Heilig, G. H. J.; Nederlof, M. M.; van Loosdrecht, M. C. M.; Stams, A. J. M.; Euverink, G. J. W. Molecular characterization of the bacterial communities in the different compartments of a full-scale reverse-osmosis water purification plant. *Appl. Environ. Microbiol.* **2008**, *74*, 5297−5304.

(12) Pang, C. M.; Liu, W.-T. Community structure analysis of reverse osmosis membrane biofilms and the significance of Rhizobiales bacteria in biofouling. *Environ. Sci. Technol.* **2007**, *41*, 4728−4734.

(13) Bereschenko, L. A.; Stams, A. J. M.; Euverink, G. J. W.; van Loosdrecht, M. C. M. Biofilm formation on reverse osmosis membranes is initiated and dominated by *Sphingomonas* spp. *Appl. Environ. Microbiol.* **2010**, *76*, 2623−2632.

(14) Gutman, J.; Herzberg, M.; Walker, S. L. Biofouling of reverse osmosis membranes: Positively contributing factors of *Sphingomonas*. *Environ. Sci. Technol.* **2014**, *48*, 13941−13950.

(15) Kawasaki, S.; Moriguchi, R.; Sekiya, K.; Nakai, T.; Ono, E.; Kume, K.; Kawahara, K. The cell envelope structure of the lipopolysaccharide-lacking gram-negative bacterium *Sphingomonas paucimobilis*. *J. Bacteriol.* **1994**, *176*, 284−290.

(16) Habimana, O.; Semião, A. J. C.; Casey, E. The role of cell-surface interactions in bacterial initial adhesion and consequent biofilm formation on nanofiltration/reverse osmosis membranes. *J. Membr. Sci.* **2014**, *454*, 82−96.

(17) Busscher, H.; Weerkamp, A. H. Specific and non-specific interactions in bacterial adhesion to solid substrata. *FEMS Microbiol. Lett.* **1987**, *46*, 165−173.

(18) Kaufman, Y.; Kasher, R.; Lammertink, R. G. H.; Freger, V. Microfluidic NF/RO separation: Cell design, performance and application. *J. Membr. Sci.* **2012**, *396*, 67−73.

(19) Kawahara, K.; Seydel, U.; Matsuura, M.; Danbara, H.; Rietschel, E. T.; Zähringer, U. Chemical structure of glycosphingolipids isolated from *Sphingomonas paucimobilis*. *FEBS Lett.* **1991**, *292*, 107−110.

(20) Gutman, J.; Kaufman, Y.; Kawahara, K.; Walker, S. L.; Freger, V.; Herzberg, M. Interactions of glycosphingolipids and lipopolysaccharides with silica and polyamide surfaces: Adsorption and viscoelastic properties. *Biomacromolecules* **2014**, *15*, 2128−2137.

(21) Hoek, E. M. V.; Elimelech, M. Cake-enhanced concentration polarization: A new fouling mechanism for salt-rejecting membranes. *Environ. Sci. Technol.* **2003**, *37*, 5581−5588.

(22) Herzberg, M.; Elimelech, M. Biofouling of reverse osmosis membranes: Role of biofilm-enhanced osmotic pressure. *J. Membr. Sci.* **2007**, *295*, 11−20.

(23) Herzberg, M.; Kang, S.; Elimelech, M. Role of Extracellular Polymeric Substances (EPS) in Biofouling of Reverse Osmosis Membranes. *Environ. Sci. Technol.* **2009**, *43*, 4393−4398.

(24) Tang, C. Y.; Chong, T. H.; Fane, A. G. Colloidal interactions and fouling of NF and RO membranes: A review. *Adv. Colloid Interface Sci.* **2011**, *164*, 126−143.

(25) Wang, X.-M.; Waite, T. D. Role of gelling soluble and colloidal microbial products in membrane fouling. *Environ. Sci. Technol.* **2009**, *43*, 9341−9347.

(26) Xu, P.; Drewes, J. E.; Kim, T.-U.; Bellona, C.; Amy, G. Effect of membrane fouling on transport of organic contaminants in NF/RO membrane applications. *J. Membr. Sci.* **2006**, *279*, 165−175.

DOI: 10.1021/ez500409h
Environ. Sci. Technol. Lett. XXXX, XXX, XXX−XXX